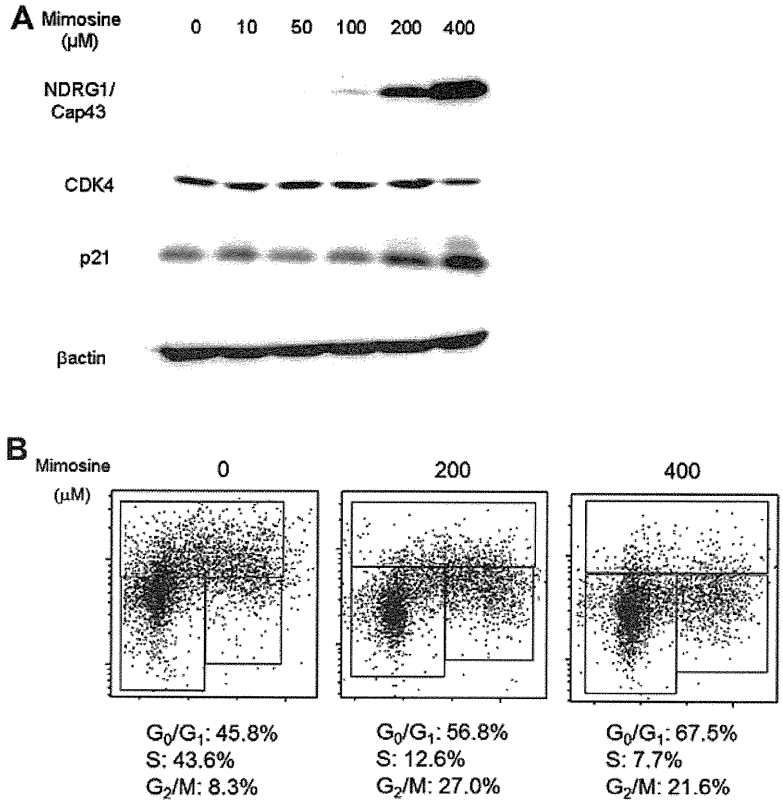

Fig. 3. Mimosine treatment in culture cell. (A) Dose-dependent study with different concentrations of mimosine for 24 h. NDRG1/Cap43 was induced when treated with 200 μM and 400 μM of mimosine. Mimosine induced p21 expression at 200 μM and 400 μM and inhibited CDK4 expression at 400 μM. (B) Cell cycle analysis with or without mimosine. Cell cycle was arrested at the G_0/G_1 phase when treated with 200 μM and 400 μM of mimosine.

NDRG1/Cap43 showed growth suppression in HCC cells *in vitro* and *in vivo*, consistent with the findings of previous studies [14,23]. Cell-cell contact often induces cell cycle arrest at the G_0/G_1 phase, through nuclear localization of p21 [24,25]. Suppressive expression of p21 was also observed in KIM-1/Mock tumor with increased expression of CDK4 as compared with KIM-1/Cap43 tumor. Expression of p21 was enhanced in KIM-1/Cap43 *in vitro* under the confluent culture condition. NDRG1/Cap43 may thus induce cell cycle arrest of HCC cells at G_0/G_1 through up-regulation of this key cell cycle regulator, p21. Several studies have documented the intranuclear p21 in senescent hepatocytes in many forms of chronic liver disease [26–30]. However, how p21 could be associated with the cell cycle growth arrest by hepatocyte remains unclear. Further study is required to determine whether NDRG1/Cap43 is involved in senescence of hepatocytes in liver diseases.

CDK4 is a cyclin dependent kinase composed of approximately 20 species. Microarray analysis of HCC revealed the patient population with low survival had high expression of CDK4 suggesting that CDK4 is a prognosis biomarker for HCC [31]. In the early G_1 phase, CDK4 and/or CDK6 are activated by D-type cyclin and initiate phosphorylation of retinoblastoma protein family [32,33]. This leads to the release of E2F transcription factors and results in the activation and transcription of E2F responsive genes required for cell cycle progression [34,35]. Cell cycle arrest at the G_0/G_1 phase is mediated by Cip/Kip families and/or Ink4a activation, followed by CDKs reduction [36]. Although the expression of p21 was up-regulated under confluent culture condition, that of CDK4 was not apparently changed in our present study (Fig. 2C). By contrast, increased expression of p21 and reduced expression of CDK4 were observed by mimosine treatment *in vitro*, and also in mouse xenograft tumor (Figs. 3A and 4C). Independent studies have reported that treatment with mimosine, a specific G_1 blocker resulted in marked up-regulation of NDRG1/Cap43 and down-regulation of CDK4 in other human cancer cell line in culture [37,38]. In HCC cells, treatment of mimosine at 200 μM and 400 μM induced expression of p21 and NDRG1/Cap43 while expression of CDK4 was decreased only when treated with 400 μM of mimosine (Fig. 3A). Induction of a certain amount of p21 by NDRG1/Cap43 might be a prerequisite for down regulation for CDK4. Since NDRG1/Cap43 expression is often up-regulated at the G_1 and G_2/M-phase but down-regulated in the S-phase of cancer cells [4], NDRG1/Cap43 may play a critical role in G_0/G_1 arrest possibly through altered expression of p21 and CDK4.

Ki-67 is a representative proliferation marker of tumor cells. Ki-67 expression is found throughout the cell cycle in the G_1, S and G_2/M phase and absent in the G_0 phase. In HCC, a high Ki-67 index was also associated with high histological grade, vascular invasion and advanced tumor

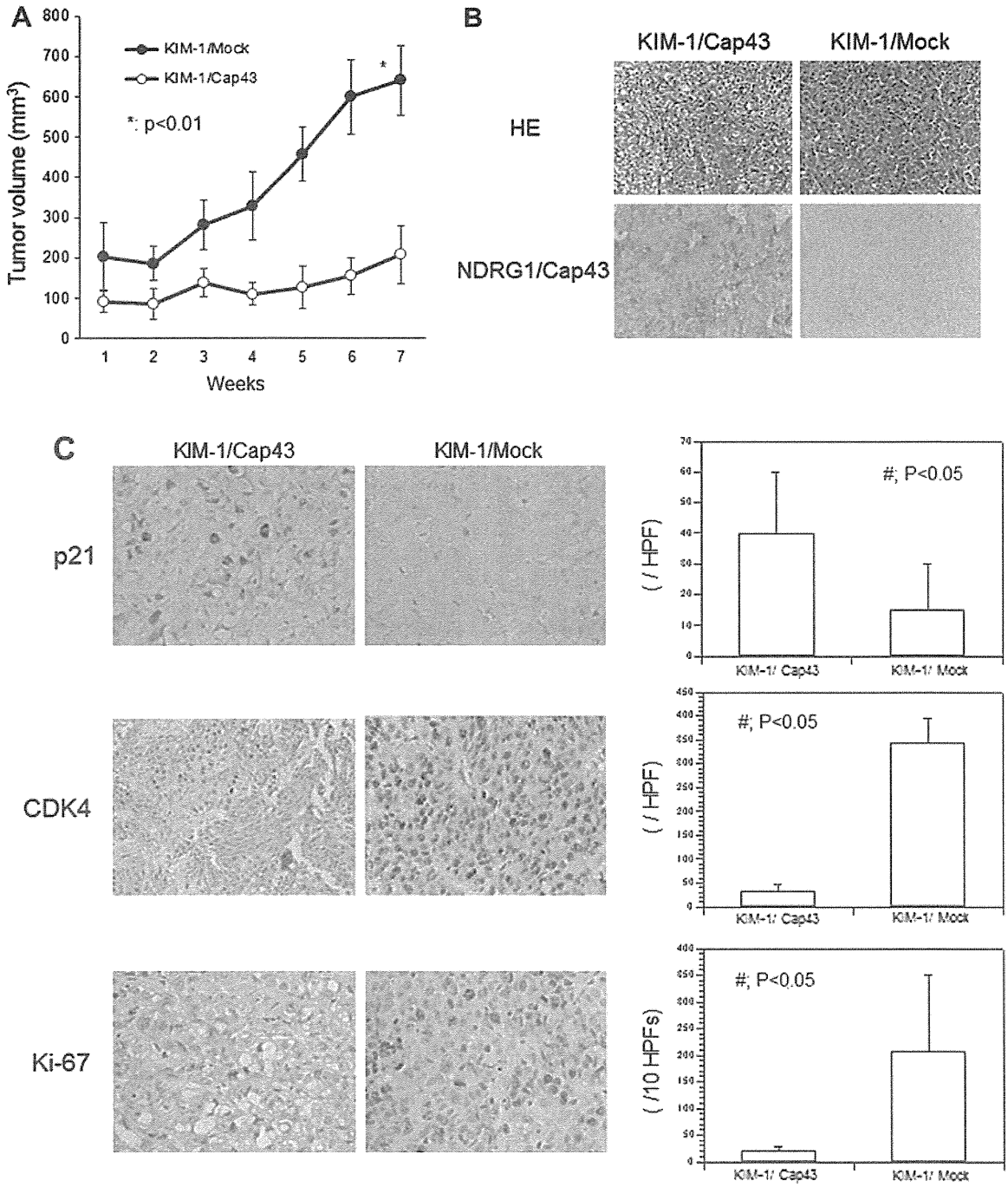

Fig. 4. Comparison of tumor growth and morphological findings between NDRG1/Cap43 and mock transfectants *in vivo*. (A) Tumor volumes were measured every week after tumor implantation. Tumor growth of KIM-1/Cap43 showed markedly reduced rates as compared with its mock-transfected line, KIM-1/Mock ($n = 6$ mice each). (B) No morphological differences were observed between NDRG1/Cap43 and mock transfectants. NDRG1/Cap43 expression was confirmed in the xenograft of NDRG1/Cap43 transfectant (magnification 200×). (C) Immunohistochemical staining of p21, CDK4 and ki-67 in mouse xenograft. The expression of all cell cycle regulators examined here was located in nucleus. The number of p21 positive cells was significantly higher in the tumor of KIM-1/Cap43 ($P < 0.05$). The number of CDK4 positive cells was significantly lower in the tumor of KIM-1/Cap43 ($P < 0.05$). Ki-67 expression was significantly lower in the tumor of KIM-1/Cap43 ($P < 0.05$) (magnification 200×).

stage [39]. In our xenograft model, high Ki-67 expression was observed in tumor without NDRG1/Cap43 expression compared with tumor generated from NDRG1/Cap43 expression, suggesting that the great number of tumor cells with NDRG1/Cap43 expression tends to be in the G_0 (or G_0/G_1) phase. Taken together, NDRG1/Cap43 might

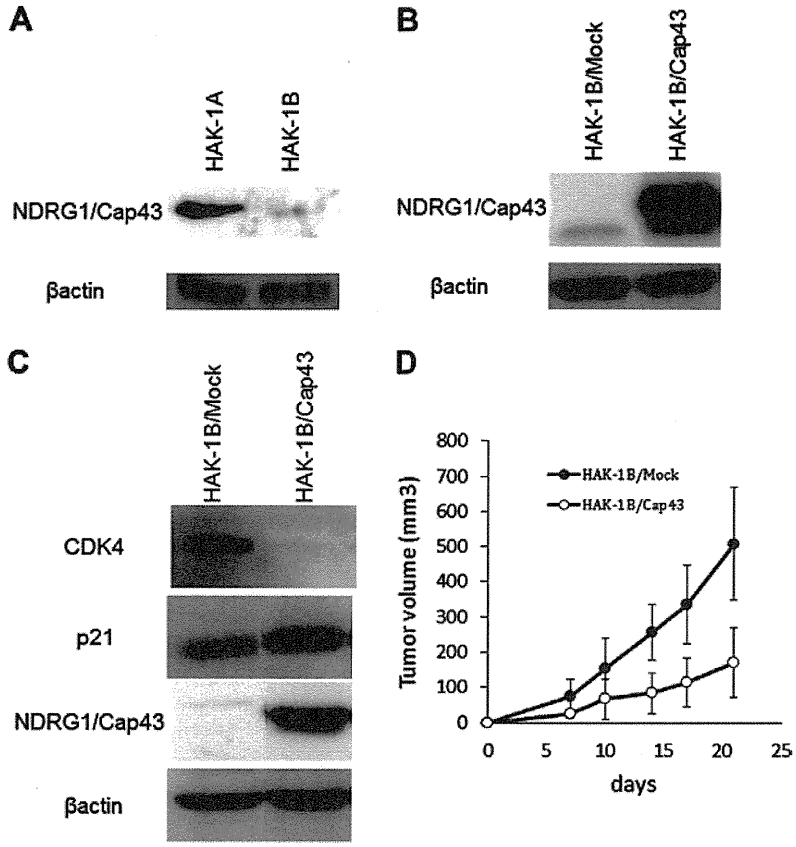

Fig. 5. (A) Expression of NDRG1/Cap43 in HAK-1A and HAK-1B examined by Western blot analysis. HAK-1A had apparent NDRG1/Cap43 expression, while HAK-1B had very low NDRG1/Cap43 expression. (B) Expression of NDRG1/Cap43 in HAK-1B/Cap43 and lack of NDRG1/Cap43 expression in HAK-1B/Mock were determined by Western blot analysis. (C) Induction of p21 and reduction of CDK4 were observed in HAK-1B/Cap43 under confluent culture condition. (D) Comparison of tumor growth between NDRG1/Cap43 and mock transfectants *in vivo*. Tumor volumes were measured every 3 days. Tumor growth of HAK-1B/Cap43 showed markedly reduced rates as compared with its mock transfected line, HAK-1B/Mock ($n = 4$ mice each).

attenuate activation of p21, leading to decreased expression of CDK4, resulting in cell cycle arrest at the G_0/G_1 phase (Fig. 6).

On the other hand, our previous study demonstrated the suppressive effect of NDRG1/Cap43 on tumor growth by pancreas cancer cells [14]. As the underlying mechanism for tumor suppressive effect, NDRG1/Cap43 overexpression was accompanied by reduced expression of IκBα and pIκBα in pancreas cancer cells [23,40]. Consistent with these previous reports, our present study demonstrated reduced expression of both IκBα and pIκBα in KIM-1/Cap43 as compared with KIM-1/Mock. NDRG1/Cap43-induced tumor suppressive effect might be in part due to the decreased NF-κB signaling pathway in HCC cells.

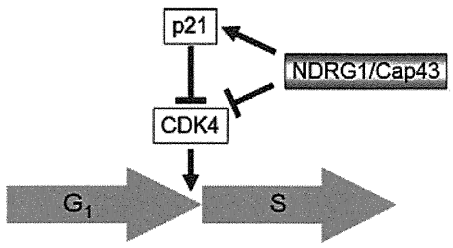

Fig. 6. Our hypothetical model of how NDRG1/Cap43 regulates cell cycle arrest at the G_0/G_1 phase. NDRG1/Cap43 attenuated activation of p21, leading to decreased expression of CDK4. NDRG1/Cap43 might thus mediate cell cycle arrest at the G_0/G_1 phase.

Based on our present study, NDRG1/Cap43-induced down-regulation of cell growth-related genes may be preferably involved in the tumor growth suppression by NDRG1/Cap43 overexpression. On the other hand, two research groups including ours have reported that NDRG1/Cap43 was related to the aggressive behavior and poor prognosis in human HCC tissues [18,19]. Yan and colleagues noted that NDRG1/Cap43 had a promoting effect on the proliferation and invasion of HCC cell lines [20]. Although there was no mechanism underlying why NDRG1/Cap43 promotes growth and malignancy by HCC cells in these studies, these results contrast with our present findings that NDRG1/Cap43 had an inhibitory effect on tumor growth of the HCC cell line. The reason for the discrepancy among these studies remains unknown at present, and further more precise studies are required to clarify the discrepancy.

In conclusion, this study has shown that NDRG1/Cap43 induces G_0/G_1-phase cell cycle arrest in HCC cell lines, and thereby exhibits an inhibitory effect on tumor growth,

suggesting that cell cycle regulators such as p21 and CDK4 might be involved in NDRG1/Cap43-induced cell cycle arrest. NDRG1/Cap43 might be a novel biomarker for developing an anticancer therapeutic strategy for HCC.

Conflicts of interest

None declared.

Acknowledgements

We thank Ms. Akemi Fujiyosi, Sachiyo Maeda and Akiko Tanaka for their excellent technical assistance and Ms. Yasuko Higuchi and Ms. Hisae Yoshioka for manuscript preparation.

References

[1] Y. Tanaka, K. Hanada, M. Mizokami, A.E. Yeo, J.W. Shih, T. Gojobori, H.J. Alter, A comparison of the molecular clock of hepatitis C virus in the United States and Japan predicts that hepatocellular carcinoma incidence in the United States will increase over the next two decades, Proc. Natl. Acad. Sci. USA 99 (2002) 15584–15589.
[2] M. Kudo, Early detection and curative treatment of early-stage hepatocellular carcinoma, Clin. Gastroenterol. Hepatol. 3 (2005) 144–148.
[3] K. Kokame, H. Kato, T. Miyata, Homocysteine-respondent genes in vascular endothelial cells identified by differential display analysis: GRP78/BiP and novel genes, J. Biol. Chem. 271 (1996) 29659–29665.
[4] S.K. Kurdistani, P. Arizti, C.L. Reimer, M.M. Sugrue, S.A. Aaronson, S.W. Lee, Inhibition of tumor cell growth by RTP/rit42 and its responsiveness to p53 and DNA damage, Cancer Res. 58 (1998) 4439–4444.
[5] D. Zhou, K. Salnikow, M. Costa, Cap43, a novel gene specifically induced by Ni2+ compounds, Cancer Res. 58 (1998) 2182–2189.
[6] A. Shimono, T. Okuda, H. Kondoh, N-myc-dependent repression of ndr1, a gene identified by direct subtraction of whole mouse embryo cDNAs between wild type and N-myc mutant, Mech. Dev. 83 (1999) 39–52.
[7] K. Masuda, M. Ono, M. Okamoto, W. Morikawa, M. Otsubo, T. Migita, M. Tsuneyoshi, H. Okuda, T. Shuin, S. Naito, M. Kuwano, Downregulation of Cap43 gene by von Hippel-Lindau tumor suppressor protein in human renal cancer cells, Int. J. Cancer 105 (2003) 803–810.
[8] E. Gomez-Casero, M. Navarro, M.L. Rodriguez-Puebla, F. Larcher, J.M. Paramio, C.J. Conti, J.L. Jorcano, Regulation of the differentiation-related gene Drg-1 during mouse skin carcinogenesis, Mol. Carcinogen. 32 (2001) 100–109.
[9] T. Okuda, Y. Higashi, K. Kokame, C. Tanaka, H. Kondoh, T. Miyata, Ndrg1-deficient mice exhibit a progressive demyelinating disorder of peripheral nerves, Mol. Cell Biol. 24 (2004) 3949–3956.
[10] B. Chen, D.M. Nelson, Y. Sadovsky, N-myc down-regulated gene 1 modulates the response of term human trophoblasts to hypoxic injury, J. Biol. Chem. 281 (2006) 2764–2772.
[11] P. Lachat, P. Shaw, S. Gebhard, N. van Belzen, P. Chaubert, F.T. Bosman, Expression of NDRG1, a differentiation-related gene, in human tissue, Histochem. Cell Biol. 118 (2002) 399–408.
[12] S. Bandyopadhyay, S.K. Pai, S.C. Gross, S. Hirota, S. Hosobe, K. Miura, K. Saito, T. Commes, S. Hayashi, M. Watabe, K. Watabe, The Drg-1 gene suppresses tumor metastasis in prostate cancer, Cancer Res. 63 (2003) 1731–1736.
[13] S. Bandyopadhyay, S.K. Pai, S. Hirota, S. Hosobe, Y. Takano, K. Saito, D. Piquemal, T. Commes, M. Watabe, S.C. Gross, Y. Wang, S. Ran, K. Watabe, Role of the putative tumor metastasis suppressor gene Drg-1 in breast cancer progression, Oncogene 23 (2004) 5675–5681.
[14] Y. Maruyama, M. Ono, A. Kawahara, T. Yokoyama, Y. Basaki, M. Kage, S. Aoyagi, H. Kinoshita, M. Kuwano, Tumor growth suppression in pancreatic cancer by a putative metastasis suppressor gene Cap43/NDRG1/Drg-1 through modulation of angiogenesis, Cancer Res. 66 (2006) 6233–6242.
[15] R.J. Guan, H.L. Ford, Y. Fu, Y. Li, L.M. Shaw, A.B. Pardee, Drg-1 as a differentiation-related, putative metastatic suppressor gene in human colon cancer, Cancer Res. 60 (2000) 749–755.
[16] M.A. Shah, N. Kemeny, A. Hummer, M. Drobnjak, M. Motwani, C. Cordon-Cardo, M. Gonen, G.K. Schwartz, Drg1 expression in 131 colorectal liver metastases: correlation with clinical variables and patient outcomes, Clin. Cancer Res. 11 (2005) 3296–3302.
[17] S. Nishio, K. Ushijima, N. Tsuda, S. Takemoto, K. Kawano, T. Yamaguchi, N. Nishida, T. Kakuma, H. Tsuda, T. Kasamatsu, Y. Sasajima, M. Kage, M. Kuwano, T. Kamura, Cap43/NDRG1/Drg-1 is a molecular target for angiogenesis and a prognostic indicator in cervical adenocarcinoma, Cancer Lett. 264 (2008) 36–43.
[18] M.S. Chua, H. Sun, S.T. Cheung, V. Mason, J. Higgins, D.T. Ross, S.T. Fan, S. So, Overexpression of NDRG1 is an indicator of poor prognosis in hepatocellular carcinoma, Mod. Pathol. 20 (2007) 76–83.
[19] J. Akiba, S. Ogasawara, A. Kawahara, N. Nishida, S. Sanada, F. Moriya, M. Kuwano, O. Nakashima, H. Yano, N-myc downstream regulated gene 1 (NDRG1)/Cap43 enhances portal vein invasion and intrahepatic metastasis in human hepatocellular carcinoma, Oncol. Rep. 20 (2008) 1329–1335.
[20] X. Yan, M.S. Chua, H. Sun, S. So, N-Myc down-regulated gene 1 mediates proliferation, invasion, and apoptosis of hepatocellular carcinoma cells, Cancer Lett. 262 (2008) 133–142.
[21] A. Kawahara, K. Azuma, S. Hattori, K. Nakashima, Y. Basaki, J. Akiba, S. Takamori, H. Aizawa, T. Yanagawa, H. Izumi, K. Kohno, S. Kono, M. Kage, M. Kuwano, M. Ono, The close correlation between 8-hydroxy-2'-deoxyguanosine and epidermal growth factor receptor activating mutation in non-small cell lung cancer, Hum. Pathol. 41 (2010) 51–959.
[22] H. Yano, A. Iemura, K. Fukuda, H. Mizoguchi, M. Haramaki, M. Kojiro, Establishment of two distinct human hepatocellular carcinoma cell lines from a single nodule showing clonal dedifferentiation of cancer cells, Hepatology 18 (1993) 320–327.
[23] F. Hosoi, H. Izumi, A. Kawahara, Y. Murakami, H. Kinoshita, M. Kage, K. Nishio, K. Kohno, M. Kuwano, M. Ono, N-myc downstream regulated gene 1/Cap43 suppresses tumor growth and angiogenesis of pancreatic cancer through attenuation of inhibitor of kappaB kinase beta expression, Cancer Res. 69 (2009) 983–4991.
[24] M. Küppers, C. Ittrich, D. Faust, C. Dietrich, The transcriptional programme of contact-inhibition, J. Cell. Biochem. 110 (2010) 234–1243.
[25] M.G. Ritt, J. Mayor, J. Wojcieszyn, R. Smith, C.L. Barton, J.F. Modiano, Sustained nuclear localization of p21/WAF-1 upon growth arrest induced by contact inhibition, Cancer Lett. 158 (2000) 73–84.
[26] V. Paradis, N. Youssef, D. Dargère, N. Ba, F. Bonvoust, J. Deschatrette, P. Bedossa, Replicative senescence in normal liver, chronic hepatitis C, and hepatocellular carcinomas, Hum. Pathol. 32 (2001) 327–332.
[27] J.G. Lunz 3rd, H. Tsuji, I. Nozaki, N. Murase, A.J. Demetris, An inhibitor of cyclin-dependent kinase, stress-induced p21Waf-1/Cip-1, mediates hepatocyte mito-inhibition during the evolution of cirrhosis, Hepatology 41 (2006) 262–1271.
[28] H. Wagayama, K. Shiraki, T. Yamanaka, K. Sugimoto, T. Ito, K. Fujisawa, K. Takase, T. Nakano, p21WAF1/CTP1 expression and hepatitis virus type, Dig. Dis. Sci. 46 (2001) 074–2079.
[29] S.U. Wiemann, A. Satyanarayàna, M. Tsahuridu, H.L. Tillmann, L. Zender, J. Klempnauer, P. Flemming, S. Franco, M.A. Blasco, M.P. Manns, K.L. Rudolph, Hepatocyte telomere shortening and senescence are general markers of human liver cirrhosis, FASEB J. 16 (2002) 35–942.
[30] A. Marshall, S. Rushbrook, S.E. Davies, L.S. Morris, I.S. Scott, S.L. Vowler, N. Coleman, G. Alexander, Relation between hepatocyte G1 arrest, impaired hepatic regeneration, and fibrosis in chronic hepatitis C virus infection, Gastroenterology 128 (2005) 33–42.
[31] J.S. Lee, I.S. Chu, J. Heo, D.F. Calvisi, Z. Sun, T. Roskams, A. Durnez, A.J. Demetris, S.S. Thorgeirsson, Classification and prediction of survival in hepatocellular carcinoma by gene expression profiling, Hepatology 40 (2004) 667–676.
[32] C.J. Sherr, J.M. Roberts, CDK inhibitors: positive and negative regulators of G1-phase progression, Genes Dev. 13 (1999) 1501–1512.
[33] C.J. Sherr, J.M. Roberts, Living with or without cyclins and cyclin-dependent kinases, Genes Dev. 18 (2004) 2699–2711.
[34] R.A. Weinberg, The retinoblastoma protein and cell cycle control, Cell 81 (1995) 323–330.
[35] N. Dyson, The regulation of E2F by pRB-family proteins, Genes Dev. 12 (1998) 2245–2262.
[36] T. Abbas, A. Dutta, p21 in cancer: intricate networks and multiple activities, Nat. Rev. Cancer 9 (2009) 00–414.
[37] Z. Dong, R.J. Arnold, Y. Yang, M.H. Park, P. Hrncirova, Y. Mechref, M.V. Novotny, J.T. Zhang, Modulation of differentiation-related gene 1

expression by cell cycle blocker mimosine, revealed by proteomic analysis, Mol. Cell Proteomics 4 (2005) 993–1001.
[38] K.S. Kulp, S.L. Green, P.R. Vulliet, Iron deprivation inhibits cyclin-dependent kinase activity and decreases cyclin D/CDK4 protein levels in asynchronous MDA-MB-453 human breast cancer cells, Exp. Cell Res. 229 (1996) 0–68.
[39] E. Kitamura, E. Hatano, T. Higashi, N. Masato, S. Seo, Y. Nakamoto, K. Yamanaka, H. Nagata, K. Taura, K. Yasuchika, T. Nitta, S. Uemoto, Proliferative activity in hepatocellular carcinoma is closely correlated with glucose metabolism but not angiogenesis, J. Hepatol. 17 (2011). Epub ahead of print.
[40] Y. Murakami, F. Hosoi, H. Izumi, Y. Maruyama, H. Ureshino, K. Watari, K. Kohno, M. Kuwano, M. One, Identification of sites subjected to serine/threonine phosphorylation by SGK1 affecting N-myc downstream-regulated gene 1 (NDRG1)/Cap43-dependent suppression of angionenic CXC chemokine expression in human pancreatic cancer cells, Biochem. Biophys. Res. Commun. 396 (2010) 376–381.

NEOPLASIA
www.neoplasia.com

Volume 13 Number 3 March 2011 pp. 187–197 187

Metronomic S-1 Chemotherapy and Vandetanib: An Efficacious and Nontoxic Treatment for Hepatocellular Carcinoma[1]

Hideki Iwamoto*,†, Takuji Torimura*,†, Toru Nakamura*,†, Osamu Hashimoto*,†, Kinya Inoue*,†, Junichi Kurogi*, Takashi Niizeki*, Reiichiro Kuwahara*, Mitsuhiko Abe*, Hiromori Koga*, Hirohisa Yano‡, Robert S. Kerbel§, Takato Ueno*,† and Michio Sata*

*Division of Gastroenterology, Department of Medicine, Kurume University School of Medicine, Kurume, Japan; †Research Center for Innovative Cancer Therapy, Kurume University School of Medicine, Kurume, Japan; ‡Department of Pathology, Kurume University School of Medicine, Kurume, Japan; §Molecular and Cellular Biology Research Sunnybrook Health Sciences Centre, Toronto, Ontario, Canada

Abstract

BACKGROUND: Metronomic chemotherapy involves frequent, regular administration of cytotoxic drugs at nontoxic doses, usually without prolonged breaks. We investigated the therapeutic efficacies of metronomic S-1, an oral 5-fluorouracil prodrug, and vandetanib, an epidermal growth factor receptor and vascular endothelial growth factor (VEGF) receptor tyrosine kinase inhibitor, in models of hepatocellular carcinoma (HCC). *METHODS:* We compared anti-HCC effects and toxicity in the six treatment groups: control (untreated), maximum tolerated dose (MTD) S-1, metronomic S-1, vandetanib, MTD S-1 with vandetanib, and metronomic S-1 with vandetanib. Tumor microvessel density (MVD) and tumor apoptosis were evaluated by immunohistochemistry. The expression of VEGF and thrombospondin-1, an endogenous inhibitor of angiogenesis, was analyzed by Western blot. *RESULTS:* Metronomic S-1 significantly inhibited tumor growth, which was enhanced by combination with vandetanib. With respect to toxicities, MTD S-1 caused severe body weight loss and myelosuppression, whereas metronomic S-1 did not cause any overt toxicities. Moreover, metronomic S-1 or metronomic S-1 with vandetanib prolonged survival, the latter treatment providing the greatest benefit. Metronomic S-1 and metronomic S-1 with vandetanib decreased MVDs and increased apoptosis in tumor tissues. The expression of VEGF in tumor tissues was upregulated by vandetanib and metronomic S-1 with vandetanib, whereas the expression of thrombospondin-1 was upregulated by metronomic S-1 and metronomic S-1 with vandetanib. *CONCLUSION:* Metronomic S-1 with an antiangiogenic agent seems to be an effective and safe therapeutic strategy for HCC.

Neoplasia (2011) 13, 187–197

Introduction

Hepatocellular carcinoma (HCC) is the fifth most common solid tumor and the third leading cause of cancer-related deaths globally [1]. Although prognosis of early and intermediate stage HCC has improved owing to advances in treatments, there are few proven effective systemic therapies for advanced HCC [2]. In particular, conventional chemotherapy using cytotoxic drugs for advanced HCC has not been shown to improve survival. Almost all cases of HCC occur in patients with chronic liver disorders, such as liver cirrhosis. Patients with liver cirrhosis have liver dysfunction and also pancytopenia. These pathologies

Abbreviations: HCC, hepatocellular carcinoma; MTD, maximum tolerated dose; MVD, microvessel density; VEGF, vascular endothelial growth factor; EGF, epidermal growth factor; TSP-1, thrombospondin-1; HUVEC, human umbilical vascular endothelial cell

Address all correspondence to: Hideki Iwamoto, MD, Division of Gastroenterology, Department of Medicine, Kurume University School of Medicine, 67 Asahi-Machi, Kurume-shi, Fukuoka-ken, 830-0011, Japan. E-mail: iwamoto_hideki@med.kurume-u.ac.jp

[1]All authors agreed to the submission of this article, and there is no conflict to disclose.

Received 18 August 2010; Revised 6 December 2010; Accepted 8 December 2010

DOI 10.1593/neo.101186

limit the use of conventional chemotherapy as a treatment strategy for HCC.

Conventional chemotherapy often involves pulsatile administration schedules using maximum tolerated doses (MTDs) of cytotoxic drugs. The long break periods between therapies not only allow recovery from various toxicities, especially myelosuppression, but also provide an opportunity, unfortunately, for the drug-treated tumors to recover as well [3]. In contrast, metronomic chemotherapy is given at frequent intervals using minimally or nontoxic doses without prolonged breaks. In several preclinical studies, such metronomic protocols have shown surprisingly effective antitumor effects, despite the reduced toxicity [4–6].

S-1 is an orally novel cytotoxic 5-flurouracil (5-FU) prodrug, which consists of tegafur and two biochemical modulators, 5-chloro-2,4-dihydroxypyridine and potassium oxonate [7]. 5-Chloro-2,4-dihydroxypyridine competitively inhibits dihydropyrimidine dehydrogenase approximately 180 times more effectively than uracil. Thus, S-1 gives rise to high concentrations of 5-FU in blood and tumor tissue for long-term periods since biochemical modulation [7,8]. A drug similar to S-1, namely, UFT, has been used successfully in metronomic preclinical studies [5]. Moreover, in the clinic it has been used successfully in randomized phase 3 trials in a metronomic fashion to treat in an adjuvant manner a variety of early stage cancers, after surgery, including non–small cell lung cancer [9] and breast cancer [10]. Because S-1 is thought to be more potent than UFT with respect to the effect of biochemical modulations, one might expect a stronger antitumor effect by using S-1 [7]. In this study, we describe a method of administering metronomic S-1 to treat HCC and compare it to conventional MTD S-1 chemotherapy, either alone or with an antiangiogenic drug.

Tyrosine kinase inhibitors such as sorafenib have proven activity in HCC patients and now represent one of the few effective systemic therapies for HCC [11]. Preclinical studies have also shown that the antitumor effect of metronomic chemotherapy can be significantly enhanced by combination with vascular endothelial growth factor (VEGF) pathway targeting agents [12,13]. In this study, we show here that metronomic S-1 might be a promising therapy to consider for concurrent daily combination with an oral antiangiogenic drug, in this case, vandetanib (ZD6474; AstraZeneca Pharmaceuticals, Macclesfield, UK). Vandetanib inhibits not only the catalytic function of VEGFR-2 but also EGF receptors (EGFRs), in contrast to sorafenib or sunitinib that do not affect EGFRs [14]. We evaluated the efficacies of vandetanib alone *in vivo* for HCC-bearing mice using various hepatoma cell lines that had different expressions of EGFR (submitted for publication). EGFR is known to contribute to 5-FU drug resistance, and 5-FU is the major metabolite of S-1 [15]. Therefore, there is a rationale for drug targeting of both EGF receptors and VEGF receptors along with metronomic chemotherapy, which was the purpose of this study. Thus, we investigated the efficacy of combining with each treatment schedule of S-1 and vandetanib using two HCC cell lines, which express low or high levels of EGFR, that is, KYN-2 and Huh-7, respectively. Overall, our results suggest that the combination treatment of metronomic S-1 plus vandetanib may be useful for the therapy of HCC.

Materials and Methods

Cell Lines and Culture

In human hepatoma cell lines, Huh-7 was originally purchased from CAMBREX Bio Science Walkersville, Inc (Walkersville, MD), and KYN-2 was provided by the Department of Pathology, Kurume University School of Medicine. Cells were maintained in Dulbecco modified Eagle medium (DMEM; Gibco Invitrogen Cell Culture Co, Auckland, New Zealand) supplemented with 10% fetal bovine serum (FBS).

Human umbilical vascular endothelial cells (HUVECs) were purchased from CAMBREX Bio Science Walkersville, Inc, and maintained with endothelial cell growth medium-2 (Clonetics, San Diego, CA) containing 5% FBS.

Animals and Drugs

Male 5-week-old nude mice (BALB/c *nu/nu*) were purchased from Kyudo KK (Fukuoka, Japan). All experiments were conducted in accordance with the National Institutes of Health guidelines for the Care and Use of Laboratory Animals.

5-FU was purchased from Kyowa Hakko Kogyo Co, Ltd (Tokyo, Japan). S-1 was provided by Taiho Pharmaceutical Co, Ltd (Tokyo, Japan). S-1 consists of a mixture of tegafur, gimeracil, and oteracil at molar ratio of 1:0.4:1 in 0.5% hydroxypropylmethylcellulose (HPMC) solutions. Vandetanib (ZD6474; Zactima) was provided by AstraZeneca Pharmaceuticals (Macclesfield, UK).

In Vitro *Cell Proliferation Assay*

As the tegafur component of S-1 is physiologically converted to 5-FU in the body, we evaluated the difference of antiproliferative effects *in vitro* of 5-FU using different schedules with both hepatoma cells and HUVECs. Approximately 1000 cells in 100 μl of DMEM containing 10% FBS was added to each well of 96-well plate. After incubation for 24 hours, the medium was exchanged to the serum-containing medium with various concentrations of 5-FU (0, 1, 10, 100, 500, 1000, 10,000 ng/ml). Each cell line was exposed to 5-FU for 5 days. To evaluate the antiproliferative effect of "MTD" *versus* "metronomic" chemotherapy, exchange of the medium containing 5-FU was performed using different schedules. For the metronomic schedule, the medium containing 5-FU was exchanged daily as described previously [16]. For the MTD schedule, the medium containing 5-FU was not changed. After incubation, cell proliferation was evaluated by a tetrazolium-based assay (Cell Count Reagent SF; Nakalai Tesque, Inc, Kyoto, Japan).

Determination of the Optimal Dose for S-1 Using Metronomic Chemotherapy

We determined the optimal metronomic dose of S-1 according to a previous report, which involved evaluating different doses of a chemotherapy drug both for antitumor effects and toxicity, with the aim of determining a dose that has minimal toxicity but retains good efficacy [17]. A total of 5×10^6 Huh-7 cells were injected into the flank regions of nude mice. Therapy with different doses of S-1 was initiated when the estimated tumor volume ($0.52 \times \text{length} \times \text{width}^2$) reached 150 to 200 mm^3. Mice received S-1 orally administrated by gavage with the following agents on a daily basis for 14 days: 1) HPMC as the control group; 2) S-1, 7.5 mg/kg per day; 3) S-1, 5.0 mg/kg per day; 4) S-1, 2.5 mg/kg per day; or 5) S-1, 1.0 mg/kg per day. Tumor-bearing mice were randomly divided into groups of 10 mice. The mice were killed at day 15 after start of treatment. The inhibition rate of tumor growth (IR %) was calculated as follows: IR % = (1 − mean RTV of treatment group / mean RTV of control group) × 100, where RTV indicates the relative tumor volume: tumor volume on killing / tumor volume on initial treatment. For comparison of the toxicity in each group, mouse body weights were measured every 3 days. Peripheral leukocyte count and hemoglobin (Hb) concentrations of these mice were also measured at day 15.

Tumor Growth and Toxicity Assessment in the Subcutaneous Tumor Transplant Model

We selected as the optimal metronomic dosage for S-1, 5.0 mg/kg per day based on our aforementioned study. We selected the MTD for S-1 15 mg/kg per day for 7 days, followed by a 7-day break period, based on previous published findings [6]. To compare the antitumor effect and toxicity caused by MTD or metronomic S-1, long-term experiments were performed using the Huh-7 subcutaneous transplant model. Mice were randomly divided to six groups: 1) HPMC as the control group; 2) MTD S-1, 15 mg/kg per day p.o. for 1 week, followed by a 1-week break period for a cumulative dose of 95 mg/kg; 3) metronomic S-1, 5 mg/kg per day p.o. for 2 weeks without any break period for a cumulative dose of 70 mg/kg; 4) vandetanib 25 mg/kg per day p.o. for 2 weeks; 5) MTD S-1 with vandetanib; or 6) metronomic S-1 with vandetanib. Each group consisted of 10 mice. It is important to note that the cumulative metronomic doses were distinctly less than the cumulative MTD. In other words, whereas the schedule used was "dose-dense," it was not "dose intense." The aforementioned schedules were performed in two cycles, 4 weeks in total. Estimated tumor volumes were measured every 3 days, and all mice were killed after 4 weeks of treatment. For comparison of the toxicity in each group, mouse body weights were measured every 3 days. Peripheral leukocyte count and hemoglobin (Hb) concentrations in these mice were also measured at sacrifice.

Tumor Growth and Survival Assessment in the Orthotopic Transplant Model

We also examined tumor growth using an orthotopic liver transplant model. The mice were implanted with 2×10^6 KYN-2 cells into the left lobe liver. Mice were randomly divided into six groups, as outlined above, and therapy was initiated 7 days after implantation of tumor cells. Each group consisted of 10 mice. The mice were killed at day 29 of initial treatment, and tumor volumes were evaluated.

In addition, a survival study was also performed using the KYN-2 orthotopic transplant model for the six groups as mentioned above. Each group consisted of 10 mice. In the group for survival observation, animals were killed according to (pre)clinical signs of weakness, for example, anorexia, or greater than 20% weight loss, and days of life were recorded from initial treatment.

Immunohistochemical Staining of CD31, PCNA, and TUNEL

The sections of all tumor tissues obtained from KYN-2 orthotopic transplant model were boiled for 30 minutes by high pH target retrieval solution (DAKO Japan, Kyoto, Japan) for antigen retrieval. The sections were incubated with rabbit anti–human CD31 antibody (diluted 1:300; Abcam, Inc, Tokyo, Japan) and rabbit anti–human PCNA antibody (diluted 1:250; Abcam, Inc) at 4°C overnight. Then the avidin-biotin procedures were subsequently performed using a Vectastatin ABC Kit (Vector Laboratories, Inc, Burlingame, CA). The sections were reacted with 0.005% H_2O_2–3,3′-diaminobenzidine at room temperature for 1 minute. For quantification of microvessel density (MVD), CD31-positive vessels were counted in randomly selected 30 areas per five tumors in each treatment group at 200-fold magnification.

The terminal deoxynucleotidyl transferase–mediated dUTP nick end labeling (TUNEL) method was performed for the evaluation of apoptosis in each of the treated tumor tissues. TUNEL labeling was performed using the ApopTag Kit (Chemicon, Temecula, CA) according to the manufacturer's instructions. The stained sections of tumors of each group were reviewed, and the apoptosis index, determined by TUNEL staining, was determined by counting at least 1000 cells in five randomly selected high-power fields (magnification, ×200).

Expression of Thrombospondin-1 and VEGF in Tumor Tissues

We examined the expression of VEGF and thrombospondin-1 (TSP-1) in treated tumor tissues using Western blot analysis. TSP-1 is a known endogenous antiangiogenic protein [18]. Five samples of each treatment group and control group were loaded in equal conditions, respectively. Thirty micrograms of protein was loaded onto a NuPAGE 4% to 12% Bis-Tris gel (Invitrogen, CA). Membranes were incubated with rabbit anti–TSP-1 antibody (1:350 dilution; Abcam, Inc) or rabbit anti-VEGF antibody (1:500 dilution; Abcam, Inc) at 4°C overnight. Equal protein loading was assessed by mouse anti–β-actin antibody (1:1000 dilution; Sigma, St Louis, MO). After incubation with HRP-conjugated anti–rabbit immunoglobulin G (1:10,000 dilution; GE Healthcare UK Ltd, Buckinghamshire, UK) or HRP-conjugated anti–mouse immunoglobulin G antibody (1:5000 dilution; GE Healthcare UK Ltd) for 1 hour, immunoreactive bands were stained by an enhanced chemiluminescence Western blot analysis system using LAS 4000 mini (Fujifilm, Tokyo, Japan) and were calculated with the amount of luminescence in each sample using multigauge software (Fujifilm). The relative amount of luminescence in each treatment group for the control group was expressed as [(treatment group VEGF or TSP-1 / treatment group β-actin) / (control group VEGF or TSP-1 / control group β-actin)] and compared with each group.

Statistical Analysis

All experimental data were expressed as mean ± SD. Differences between groups were examined for statistical significance using the Mann-Whitney *U* test, the Kruskal-Wallis test, and nonparametric analysis of variance. If the one-way analysis of variance was significant, differences between individual groups were estimated using the Fisher least significant difference test. Overall survival was estimated according to the Kaplan-Meier method and compared using the log-rank test. $P < .05$ was considered to be statistically significant.

Results

Comparison of Antiproliferative Effects of Metronomic versus MTD Type Chemotherapy In Vitro

The 50% inhibitory concentration (IC_{50}) levels of metronomic and MTD schedules of 5-FU, the major metabolite of S-1, for each cell line are shown in Table 1. The antiproliferative effects of 5-FU for each cell line were found to be dose-dependent (Figure 1, *A–C*). The IC_{50} levels for the MTD and metronomic schedule for Huh-7 cells were 3.84 and 0.77 μM, respectively (Figure 1*A*). The IC_{50}

Table 1. IC_{50} Levels of MTD and Metronomic Schedule in Hepatoma Cell Lines and Endothelial Cell.

	5-FU IC_{50} (μM)	
	MTD	Metronomic
Hepatoma cell lines		
Huh-7	3.84	0.77
KYN-2	7.69	3.84
Endothelial cell		
HUVECs	7.7	0.76

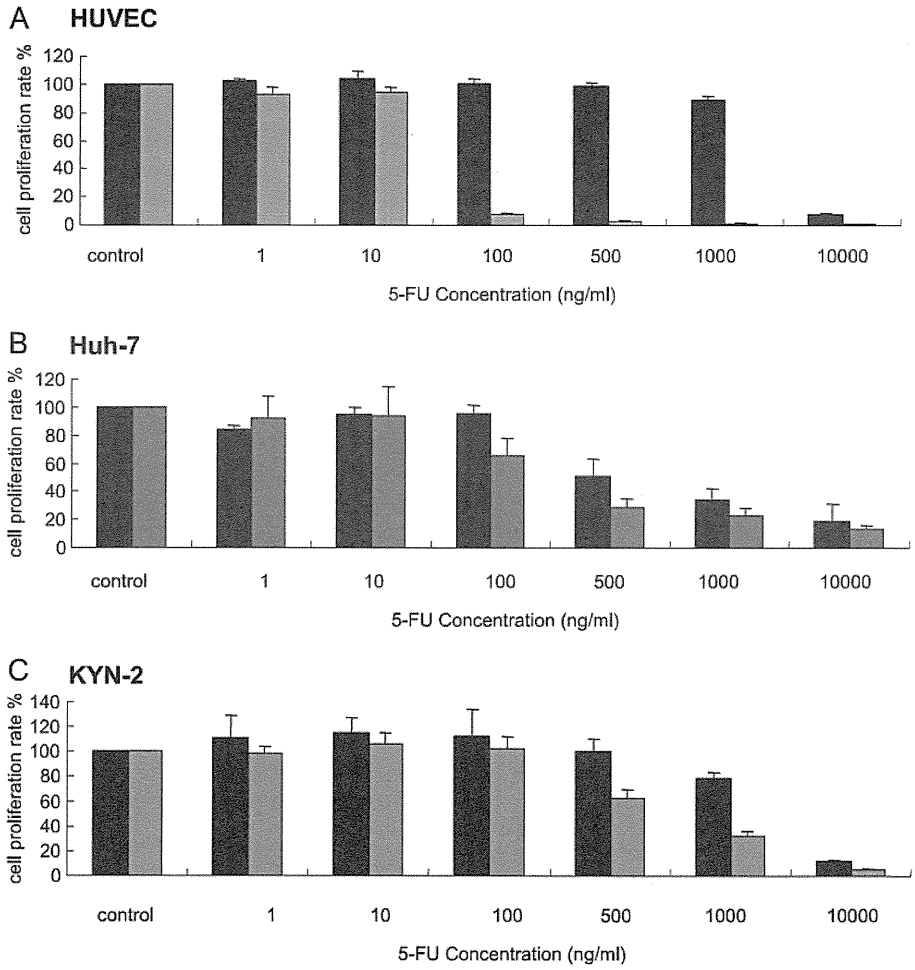

Figure 1. Inhibitory effect of metronomic chemotherapy for each cell line tested in a cell proliferation assay. To evaluate the antiproliferative effect of "MTD" and "metronomic" chemotherapy *in vitro*, exchange of the medium containing 5-FU was performed in different schedules. For the metronomic schedule, the medium containing 5-FU (0, 1, 10, 100, 500, 1000, and 10,000 ng/ml) was exchanged once a day. For the MTD schedule, the medium containing 5-FU was not changed. Data are shown as a ratio of the control and expressed as mean ± SD of 10 samples. *$P < .001$ compared with each schedule. Dark gray–shaded columns show MTD schedule, and light gray–shaded columns showed metronomic schedule. (A) HUVEC. HUVEC was cultured with 100 μl of endothelial cell growth medium-2 with 5% FBS containing 5-FU. (B) Huh-7. (C) KYN-2. Hepatoma cells were cultured with 100 μl of DMEM with 10% FBS containing 5-FU.

levels for KYN-2 were 7.69 and 3.84 μM, respectively. For the hepatoma cell lines, the metronomic schedule inhibited cell proliferation at approximately 1/2 to 1/4 concentrations of 5-FU compared with MTD schedule (Table 1). The metronomic schedule for HUVECs inhibited cell proliferation at apparently lower levels (IC_{50} levels, 0.76 μM) approximately 1/10 the concentration of 5-FU compared with MTD schedule (IC_{50} levels, 7.7 μM; Table 1).

Determination of the Optimal Dose of S-1 for Metronomic Chemotherapy In Vivo*: Maximum Tumor Growth Inhibition with Minimal Toxicity*

In the 7.5- and 5.0-mg/kg-per-day S-1 treatment groups, there were significant differences in suppression of tumor growth compared with the control group ($P < .05$; Figure 2*A*), and dosages lower than 2.5 mg/kg per day S-1 were not statistically effective compared with the control group. In addition, we evaluated body weight loss and myelosuppression toxicities associated with administration of S-1 (Figure 2, *B–D*). With respect to body weight loss, there was no significant difference between each group (Figure 2*B*). But only the 7.5-mg/kg-per-day group showed severe toxicity as determined by reductions in Hb concentration and leukocyte count ($P < .001$, compared with the control group; Figure 2, *C* and *D*). Therefore, we selected 5.0 mg/kg per day as the optimal metronomic dosage of S-1, which was used in all subsequent experiments.

Evaluation of the Antitumor Effect and Toxicity for Metronomic S-1 Chemotherapy in the Subcutaneous Transplant Tumor Model

In the assay for tumor growth, statistical differences were observed between the control group and all treatment groups (Figure 3*A*).

Metronomic S-1 potently inhibited tumor growth compared with MTD S-1 ($P < .01$). The mean tumor volumes were 4810.5 ± 1440.9 cm^3 in the control group, 3212.6 ± 1364.7 cm^3 in the MTD S-1 group, 1927.1 ± 652.9 cm^3 in the metronomic S-1 group, and 2331.4 ± 662.1 cm^3 in the vandetanib group, respectively. The mean tumor volumes in the MTD S-1 plus vandetanib group and metronomic S-1 plus vandetanib group were 2026.7 ± 1106.7 and 1383.7 ± 697.5 cm^3, respectively. The greatest inhibition of tumor growth was induced by the metronomic S-1 in combination with vandetanib (Figure 3*A*). In addition, we evaluated toxicity in each of Huh-7 subcutaneous tumor treatment groups (Figure 3, *B–D*). In leukocyte count, there were no significant differences in the groups (Figure 3*B*). In Hb concentration, the control group was 12.84 ± 1.82 g/dl, the MTD S-1 group was 9.77 ± 3.63 g/dl, the metronomic S-1 group was 11.73 ± 3.27 g/dl, and the vandetanib group was 12.34 ± 2.77 g/dl. For the combination treatments, the MTD S-1 plus vandetanib group was 8.24 ± 1.64 g/dl, and for the metronomic S-1 plus vandetanib group, it was 11.74 ± 1.55 g/dl (Figure 3*C*). With respect to rate of body weight loss, in the MTD S-1 monotherapy and MTD S-1 with vandetanib groups, the values observed were 10.48% ± 6.85% and 8.59% ± 5.02% reduction compared with the control group, respectively. Vandetanib, metronomic S-1, and the combination therapy resulted in 5.64% ± 4.23%, 3.04% ± 2.23%, and −0.51% ± 5.56% reduction compared with the control group, respectively (Figure 3*D*). Both the MTD S-1 and MTD S-1 plus vandetanib treatment groups experienced severe body weight loss and reduced Hb concentrations compared with the control group (Figure 3, *C* and *D*). In marked contrast, the metronomic S-1 monotherapy and metronomic S-1 with vandetanib groups did not manifest any overt toxicity (Figure 3, *B–D*).

Evaluation of Antitumor Efficacy Using Metronomic S-1 Chemotherapy in an Orthotopic Liver Transplant Model

For tumor volume assessments, all treatments except MTD S-1 monotherapy were effective compared with the control group (Figure 4*A*). Tumor volumes at sacrifice were 4186.0 ± 1128.0 cm^3 in the control group, 3259.0 ± 788.7 cm^3 in the MTD S-1 group, 1501.3 ± 1002.2 cm^3 in the metronomic S-1 group, and 1582.0 ± 354.9 cm^3 in the vandetanib group. There was a significant difference between metronomic S-1 and MTD S-1 in tumor growth inhibition ($P < .05$; Figure 4*A*). For the combination treatment groups, tumor volumes were 931.1 ± 331.7 cm^3 in the MTD S-1 plus vandetanib group and 875.0 ± 369.4 cm^3 in the metronomic S-1 plus vandetanib group. There was no significant difference between the metronomic S-1 plus vandetanib group and the MTD S-1 plus vandetanib group. However, the greatest inhibition of tumor growth was detected in the metronomic S-1 plus vandetanib treatment group ($P < .001$; Figure 4*A*).

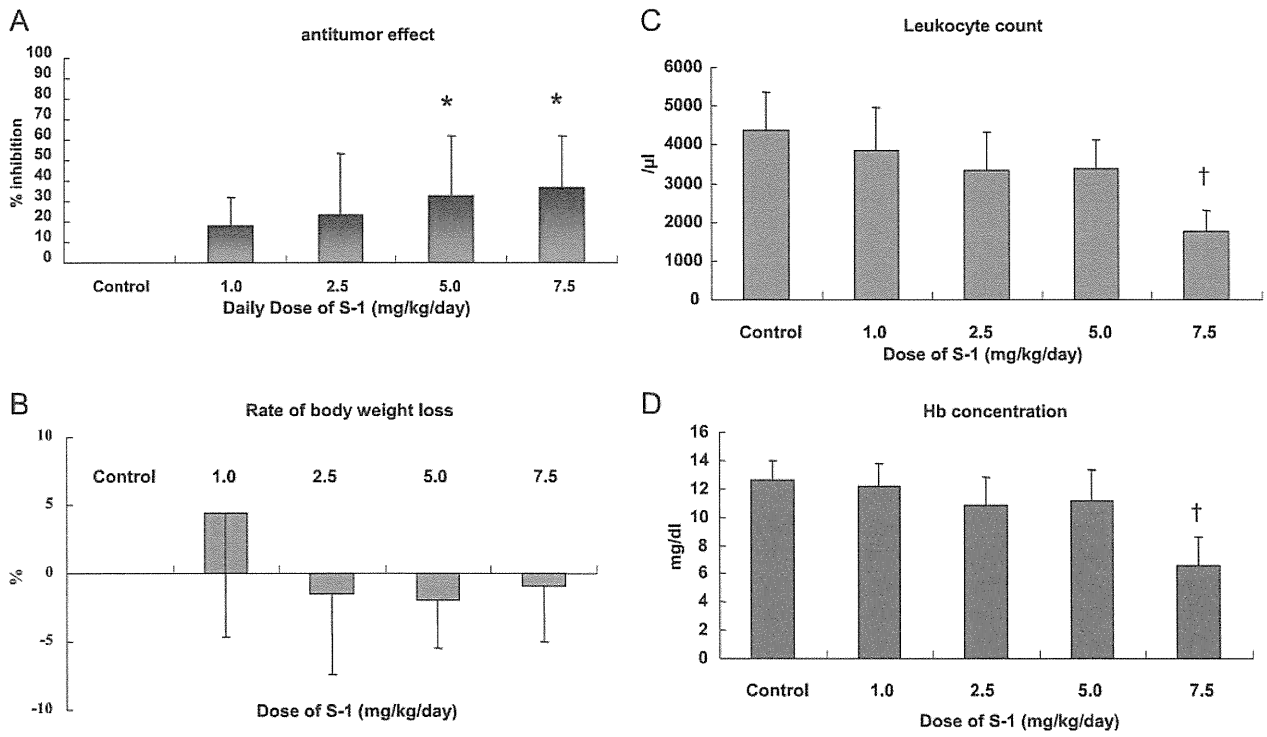

Figure 2. Determination of the optimal dose of S-1 in metronomic chemotherapy. Huh-7 subcutaneous tumor models were treated daily with either HPMC or different metronomic doses of S-1 (1.0, 2.5, 5.0, or 7.5 mg/kg per day) for 14 consecutive days. (A) Inhibition rates of tumor volumes (%) are expressed as mean ± SD ($n = 10$ per group). Dosages of 5.0 and 7.5 mg/kg per day S-1 groups statistically inhibited tumor growth compared with the control group (*$P < .05$). (B–D) Toxicity parameters are represented as mean ± SD. (B) Body weight (BW) changes on killing were calculated according to the following formula: BW change (%) = [(BW on sacrifice) − (BW on day 0)] × 100. (C) Hb concentration. (D) Leukocyte count. Each different dose of S-1 did not show body weight loss. However, the only 7.5-mg/kg-per-day S-1 group represented severe myelosuppression, such as decreased Hb concentration or leukocyte count. †$P < .001$ by compared with the control group.

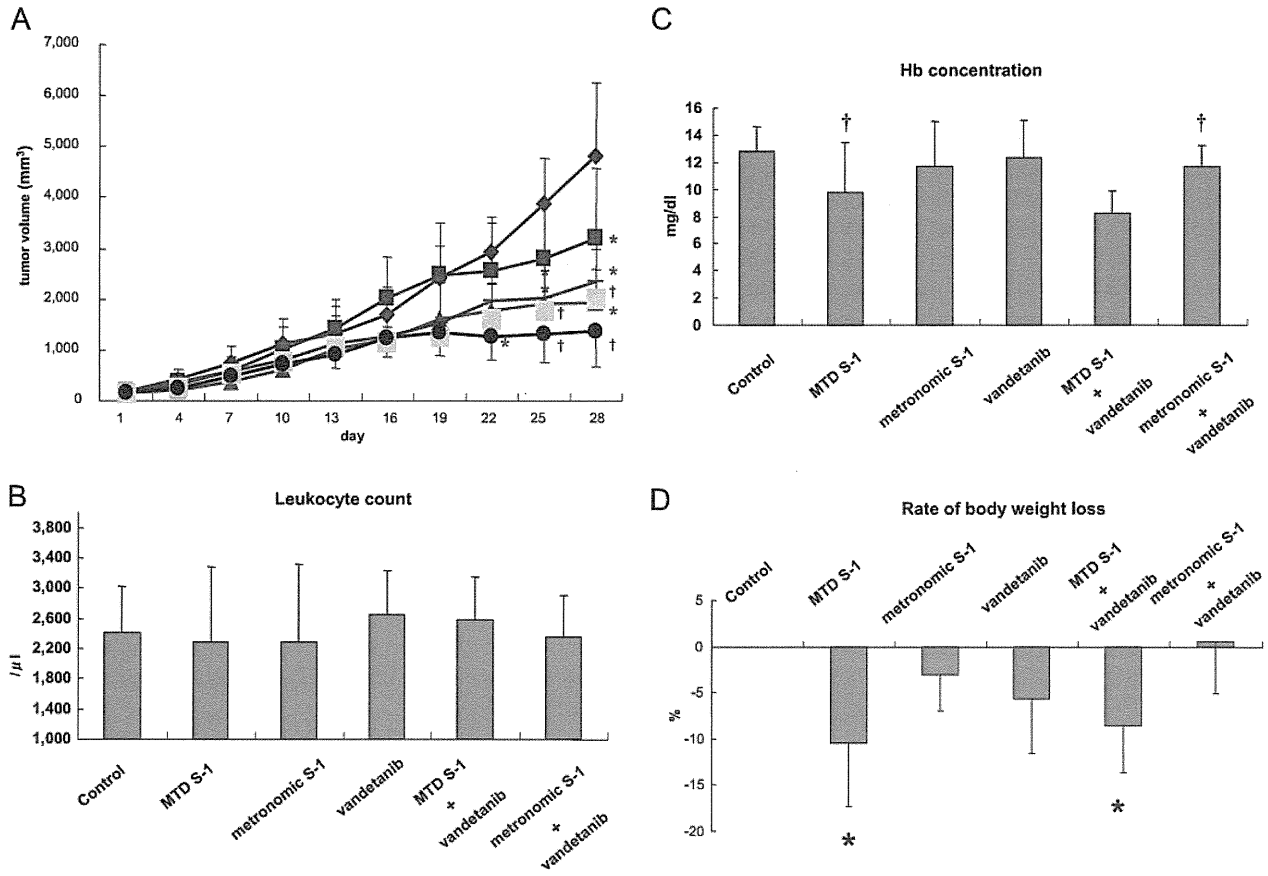

Figure 3. Therapeutic effects of metronomic S-1 chemotherapy in the Huh-7 subcutaneous tumor transplant model. (A) Tumor-bearing nude mice (n = 10 per group) were treated in the following six groups: 1) HPMC as the control group (blue); 2) MTD S-1 15 mg/kg per day for 1 week, followed by a 1-week break period (purple); 3) metronomic S-1 5 mg/kg per day for 2 weeks without break period (green); 4) vandetanib 25 mg/kg per day for 2 weeks (red); 5) MTD S-1 with vandetanib (yellow); or 6) metronomic S-1 with vandetanib (black). All treatments were performed for 4 weeks in total. Tumor volume changes are expressed as mean ± SD. All treatments showed efficacy compared with the control group (*P < .05), and the metronomic S-1 therapy was more effective than the MTD S-1 treatment. The metronomic S-1 with vandetanib significantly inhibited tumor growth compared with the control group (†P < .001). (B–D) Toxicity parameters are expressed as mean ± SD. (B) Hb concentration. (C) Leukocyte count. (D) Rate of body weight loss. MTD S-1 and the MTD S-1 with vandetanib showed severe body weight loss (*P < .01) and decreased Hb concentration (†P < .05) compared with the control group. Metronomic S-1 and the metronomic S-1 with vandetanib did not show any overt toxicities.

Evaluation of Survival Using Metronomic S-1 Chemotherapy in an Orthotopic Liver Transplant Model

The mean survival time in the control group was 28.9 ± 6.4 days. MTD S-1 did not prolong survival (mean survival time, 29.6 ± 3.9 days). In contrast, metronomic S-1 significantly prolonged survival (mean survival time, 34.3 ± 4.8 days). The mean survival time in the vandetanib group was 33.6 ± 5.0 days. MTD S-1 plus vandetanib treatment did not prolong survival times compared with vandetanib monotherapy (mean survival time, 37.6 ± 5.5 days). However, the metronomic S-1 plus vandetanib group provided the greatest prolonged survival times among all the treatment groups (mean survival time, 49.6 ± 11.5 days; Figure 4*B*).

Effect of Metronomic S-1 Chemotherapy Alone and in Combination with Vandetanib on Parameters of Tumor Angiogenesis

The results in Figure 5 show the MVD count in each treatment group. There was no significant difference in the MVD count between the control and the MTD S-1 group (control 41.1 ± 9.2, MTD S-1 35.8 ± 5.5; Figure 5*B*). However, tumor MVD was decreased in the metronomic S-1 group (17.2 ± 4.1) compared with the control group (P < .001) and the MTD S-1 group (P < .001; Figure 5*B*). Tumor MVD in mice treated with vandetanib was 13.7 ± 5.1. In the MTD S-1 plus vandetanib group, the MVD count was 18.8 ± 7.4. Metronomic S-1 plus vandetanib group showed the greatest reduction of tumor MVD (P < .01 compared with MTD S-1 plus vandetanib group, 8.2 ± 1.6; Figure 5*B*).

Detection of Proliferation and Apoptotic Cells in Tumor Tissues

To further investigate the mechanism of the observed antitumor effect, we examined the effect of metronomic S-1 and in combination with vandetanib on tumor cell proliferation and apoptosis (Figure 5). With respect to tumor cell proliferation, there were no differences between the control and all treated groups. The mean

number of apoptotic tumor cells (apoptotic index) measured in the control group was 6.2 ± 2.6. The MTD S-1 group did not show any significant difference (6.1 ± 4.9). However, the metronomic S-1 and vandetanib groups showed a significant increase in the apoptosis index (26.0 ± 5.4 and 18.4 ± 8.8, respectively, $P < .0001$). A significant increase in the tumor cell apoptosis index was also observed in the metronomic S-1 plus vandetanib group with 42 ± 3.5 ($P < .0001$).

Expression of VEGF and TSP-1 in Tumor Tissues

The results in Figure 6 show the expression of TSP-1 and VEGF in treated tumor tissues. The expression level of TSP-1 was significantly upregulated by approximately two- to three-fold in both the metronomic S-1 and the metronomic S-1 plus vandetanib treatment groups ($P < .05$ compared with the control group; Figure 6, *A* and *B*). With respect to expression levels of VEGF, there were no differences between the control and the MTD S-1 and metronomic S-1 groups (Figure 6, *C* and *D*). In contrast, the vandetanib and the metronomic S-1 plus vandetanib groups showed significantly upregulated the VEGF expression compared with the control group ($P < .05$; Figure 6, *C* and *D*). There was a significant difference between the vandetanib monotherapy group and the metronomic S-1 plus vandetanib treatment group ($P = .045$).

Discussion

Our results add to an expanding body of literature reporting the therapeutic benefit of metronomic chemotherapy, especially when it is combined concurrently with a targeted antiangiogenic drug [5,12,13]. Moreover, to our knowledge, this is the first preclinical report of using S-1 in a metronomic dosing and administration schedule for HCC preclinical model. Also noteworthy is that we undertook a comparative

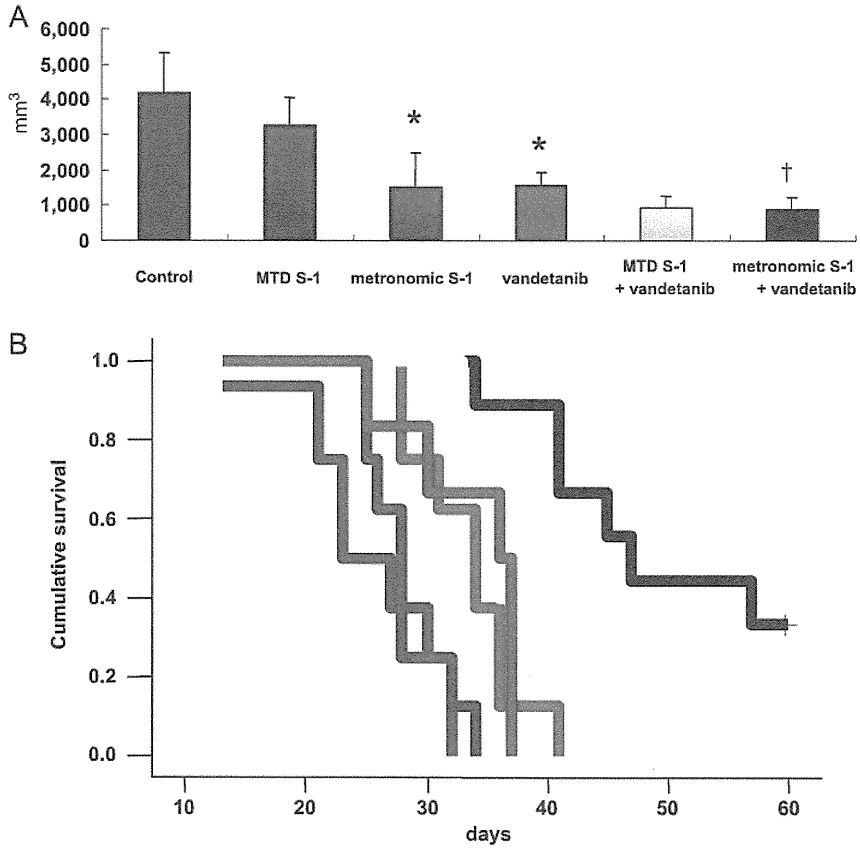

Figure 4. Assessment of therapeutic effects in KYN-2 liver transplant model. Tumor-bearing nude mice were treated in the following six groups: 1) HPMC as the control group (blue); 2) MTD S-1: 15 mg/kg per day for 1 week, followed by 1 week break period (purple); 3) metronomic S-1: 5 mg/kg per day for 2 weeks without break period (green); 4) vandetanib 25 mg/kg per day for 2 weeks (red); 5) MTD S-1 with vandetanib (yellow); or 6) metronomic S-1 with vandetanib (black). (A) Inhibition of tumor growth for KYN-2 liver transplant model. All treatments were performed 4 weeks in total. There was no significant difference between the control and the MTD S-1 groups. The metronomic S-1 group contributed to obvious inhibitory effect of tumor growth (*$P < .05$ compared with the control and the MTD S-1 groups). The metronomic S-1 with vandetanib treatment group showed the greatest inhibitory effect of tumor growth among all the groups (†$P < .001$). (B) Survival of mice treated with MTD S-1 or metronomic S-1 and in combination with vandetanib ($n = 10$ per group). Treatment was continued until mice were moribund, and days of life were recorded. Survival data were compared for significance with the log-rank test. MTD S-1 did not prolong survival compared with the control group. In contrast, metronomic S-1 prolonged survival compared with the control and MTD S-1 groups. The metronomic S-1 with vandetanib group provided the most effective therapy with longest survival times among all the groups ($P < .001$).

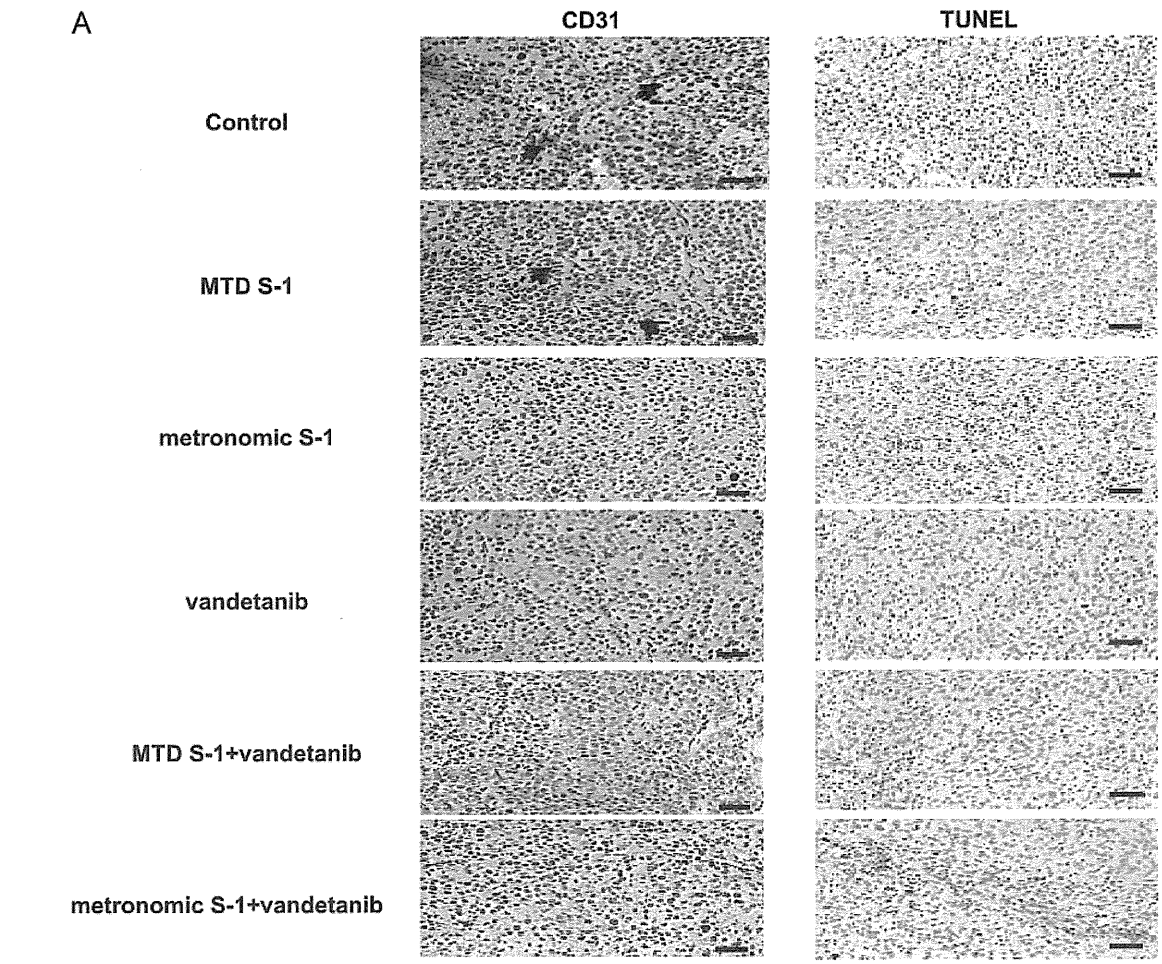
A
CD31
TUNEL
Control
MTD S-1
metronomic S-1
vandetanib
MTD S-1+vandetanib
metronomic S-1+vandetanib

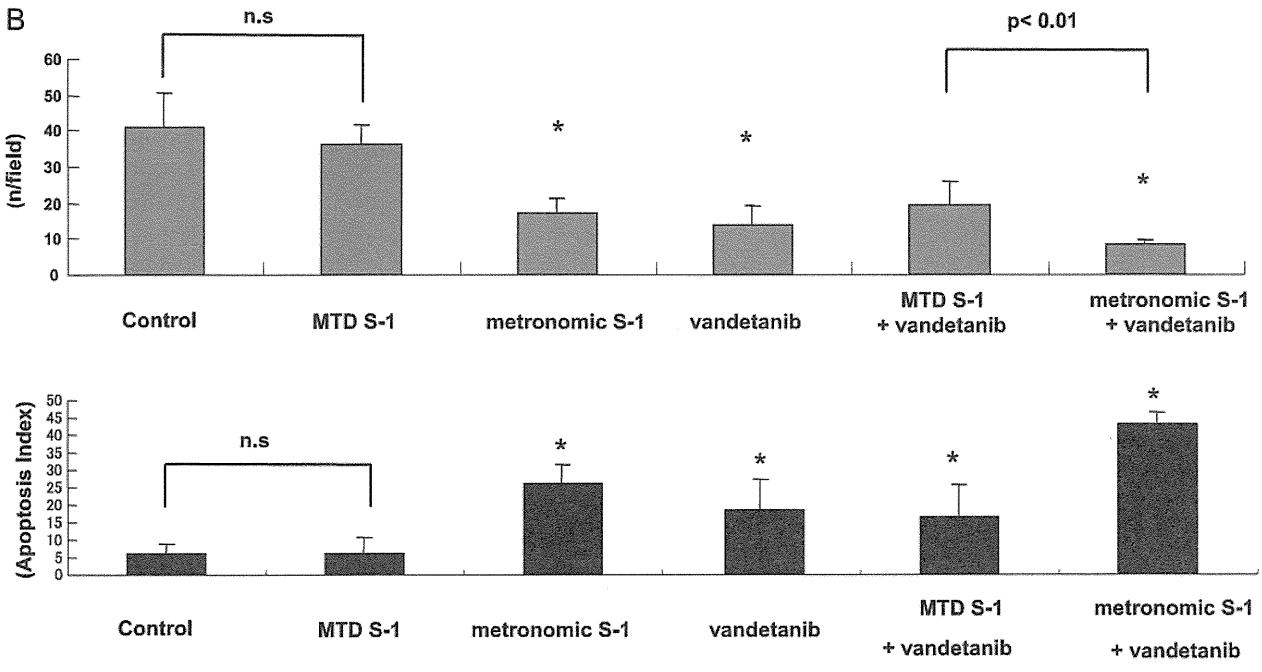
B
n.s
p< 0.01
(n/field)
60
50
40
30
20
10
0
*
Control
MTD S-1
metronomic S-1
vandetanib
MTD S-1 + vandetanib
metronomic S-1 + vandetanib
(Apoptosis Index)
50
45
40
35
30
25
20
15
10
5
0
n.s
*
Control
MTD S-1
metronomic S-1
vandetanib
MTD S-1 + vandetanib
metronomic S-1 + vandetanib

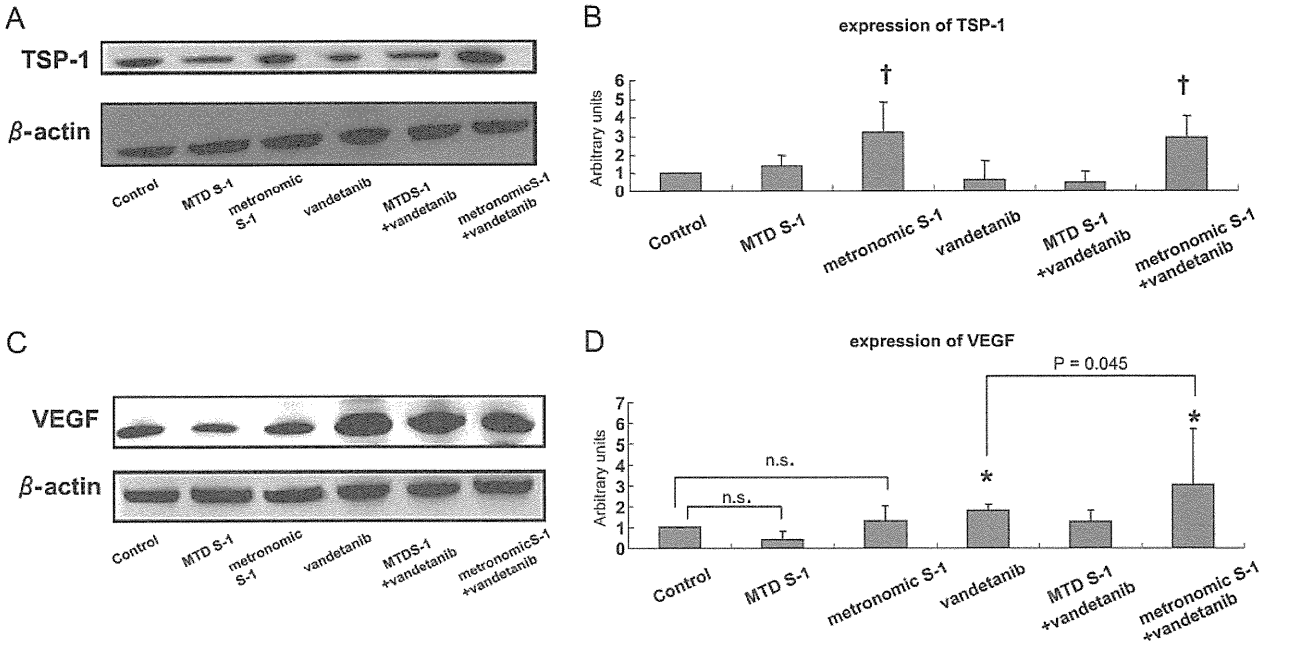

Figure 6. Western blot analysis of TSP-1 and VEGF. The band intensities of both TSP-1 and VEGF in treatment groups were measured and calibrated with each protein in control group and β-actin. (A and B) The metronomic S-1 and metronomic S-1 with vandetanib groups showed strongly upregulated the expression of TSP-1 ($^{\dagger}P < .001$ compared with the control group). (C and D) The expression of tumor VEGF was increased by the vandetanib and the metronomic S-1 with vandetanib groups. There were no differences between the control and the MTD S-1, metronomic S-1 group ($^{*}P < .05$ compared with the control group). There was a significant difference between the vandetanib and metronomic S-1 with vandetanib group ($P = .045$).

analysis of the effects of S-1 given in a more conventional MTD schedule with metronomic S-1, and our results consistently showed the metronomic dosing/schedule was superior to the MTD protocol, both in terms of increased antitumor efficacy and reduced toxicity. Importantly, in this regard, the metronomic protocol we used involved a cumulative dose over time that was 30% less than the corresponding MTD protocol. Below we discuss a number of different aspects of our results and some of the translational/clinical implications.

Antiangiogenic Effects Mediated by Metronomic S-1 Chemotherapy

Previous studies during the last decade have indicated that metronomic chemotherapy regimens using cytotoxic agents inhibit tumor growth by various mechanisms, namely, antiangiogenic effects, direct tumor cell targeting effects, or anticancer immune responses [4,19, 20]. Our results with metronomic S-1 would seem to confirm the antiangiogenic effect findings. First, we found that exposure of 5-FU in a metronomic-type protocol *in vitro* brought about a greater antiproliferative effect at distinctly low concentrations not only of 5-FU on two different tumor cell lines but also, especially, HUVECs, compared with an MTD-like exposure. This is similar to the results of other studies such as that of Bocci et al. [16] using paclitaxel or the active metabolite of cyclophosphamide. Second, we found reduced MVD and increased number of apoptotic tumor cells in mice treated with the metronomic S-1 schedule but not the MTD protocol. Third, we observed an increased expression of TSP-1, which has been reported previously using other cytotoxic drugs administered in a metronomic fashion *in vivo*, including cyclophosphamide [21]. Fourth, we noted that a tumor cell line (KYN-2) that is intrinsically resistant *in vitro* to high concentrations of 5-FU—the major metabolite of S-1—nevertheless responds to metronomic S-1 *in vivo* but not to MTD S-1, suggesting that a target other than the tumor cell population *per se* is likely involved in the *in vivo*

Figure 5. MVD and apoptosis in tumors tissues. The sections of tumors from the KYN-2 liver transplant model were stained by anti-CD31 antibody and Terminal deoxynucleotidyl transferase (TdT)–mediated dUTP nick-end labeling (TUNEL). Original magnification, ×200. The density of CD31-positive vessels (arrow) and TUNEL in a tumor field are represented as mean ± SD ($n = 30$ per group). (A) Representative sections for each treatment are shown. Bar, 10 μm. (B) There was no significant difference in MVD between the control and the MTD S-1 groups. Tumor vessel numbers were reduced by metronomic S-1. The metronomic S-1 with vandetanib group showed the most inhibitory effect of tumor vessel count among all the groups ($^{*}P < .001$ compared with the control group and the MTD S-1 group). The MTD S-1 group did not show any significant difference in the number of tumor cell apoptosis index (6.1 ± 4.9). However, the metronomic S-1 and vandetanib groups significantly increased in the number of apoptosis index, respectively (26.0 ± 5.4 and 18.4 ± 8.8, $P < .0001$). A significant increase of tumor cell apoptosis index was also observed in the metronomic S-1 with vandetanib group with 42 ± 3.5 ($P < .0001$).

antitumor activity that was observed using metronomic S-1. Fifth, O'Reilly et al. [22] have reported that the antiangiogenic effect mediated by endogenous antiangiogenic factors induces increased apoptosis of tumor cells, likely a secondary effect due to decreased MVD, whereas proliferation of tumor cells was not affected. Similarly, tumor apoptotic cell numbers were increased, whereas proliferation of tumor cells was not inhibited by metronomic S-1 chemotherapy in our study. On the basis of all of the aforementioned data and information, the antitumor effect of metronomic S-1 chemotherapy was likely to be mainly through antiangiogenesis mediated by inhibiting the proliferation of endothelial cells and inducing the expression of TSP-1, although some additional mechanisms cannot be entirely excluded. The mechanism of antiangiogenesis of metronomic S-1 chemotherapy is thought to be quite different from that of vandetanib. Inhibiting VEGFR by vandetanib resulted in increased VEGF production in tumor tissues, paradoxically, whereas metronomic S-1 chemotherapy did not increase VEGF production. Ebos et al. [23] reported that this difference of production of VEGFs influenced to achieving malignant potential of cancer cells. Also, at this point, metronomic chemotherapy is thought to be a promising strategy of long-term treatment of cancer.

Translational/Clinical Implications of the Metronomic S-1 + Vandetanib Preclinical Results

There are several potentially important implications of our results with respect to how they might conceivably be exploited for the future treatment and management of HCC patients. It is well known that there are no effective chemotherapy regimens for the treatment of advanced HCC using conventional chemotherapy regimens. One reason for this is the frequent underlying liver dysfunction [2]. As a consequence, using MTD given in conventional schedules is often contraindicated because of possible excessive toxicity. However, chemotherapy drugs given in a metronomic, less toxic fashion may be an alternative strategy to circumvent this problem. In this regard, there is conflicting evidence regarding the clinical benefit of metronomic UFT, another 5-FU prodrug, at least in the postoperative adjuvant use for HCC [24]. However, some aspects regarding the negative clinical findings should be taken into consideration. One is the dosing. The daily dose used in the aforementioned adjuvant study was less than the dose used for a positive phase 3 adjuvant UFT clinical trial for non–small cell lung cancer patients [9]. The second is the benefit that might be gained by using an antiangiogenic drug in combination with metronomic UFT. For example, a recent report by Tang et al. showed that neither metronomic UFT nor antiangiogenic drug therapy alone had overt antitumor activity in a model of locally advanced HCC, whereas these drugs when combined showed significant antitumor activity [25]. Also, in our study, combining with vandetanib resulted in enhanced antitumor effects for S-1 chemotherapy; nevertheless, MTD S-1 monotherapy did not show any effective antitumor effects. VEGFR is related to chemoresistance for tumor endothelial cells through surviving [26]. Inhibiting VEGFR by vandetanib might have contributed to enhanced chemosensitivity for tumor endothelial cells. And EGFR is associated with resistance to 5-FU [15]. Inhibiting EGFR by vandetanib might have enhanced chemosensitivity to 5-FU. In addition, it is notable in our study that not only the combination with vandetanib but also metronomic S-1 monotherapy showed significant antitumor effects. Because S-1 may be superior to UFT in antitumor effect by virtue of its biochemical modulators [7], S-1 might be an even more suitable agent for metronomic chemotherapy.

In summary, we have demonstrated preclinically that metronomic S-1 chemotherapy showed effective therapeutic outcomes without overt toxicity for treatment of HCC, mainly by suppressing tumor angiogenesis, and the activity of which is amplified by concurrent combination with vandetanib. Metronomic S-1 and the concurrent combination treatment with an antiangiogenic agent might be a promising treatment strategy for HCC.

References

[1] Parkin D, Bray F, Ferlay J, and Pisani P (2001). Estimating the world cancer burden Globocan 2000. *Int J Cancer* **94**, 153–156.

[2] Llovet J, Di Bisceglie A, Bruix J, Kramer B, Lencioni R, Zhu A, Sherman M, Schwartz M, Lotze M, Talwalkar J, et al. (2008). Design and endpoints of clinical trials in hepatocellular carcinoma. *J Natl Cancer Inst* **100**, 698–711.

[3] Kim JJ and Tannock IF (2005). Repopulation of cancer cells during therapy: an important cause of treatment failure. *Nat Rev Cancer* **5**(7), 516–525.

[4] Kerbel R and Kamen B (2004). The anti-angiogenic basis of metronomic chemotherapy. *Nat Rev Cancer* **4**, 423–436.

[5] Munoz R, Man S, Shaked Y, Lee C, Wong J, Francia G, and Kerbel R (2006). Highly efficacious nontoxic preclinical treatment for advanced metastatic breast cancer using combination oral UFT-cyclophosphamide metronomic chemotherapy. *Cancer Res* **66**, 3386–3391.

[6] Man S, Bocci G, Francia G, Green S, Jothy S, Hanahan D, Bohlen P, Hicklin D, Bergers G, and Kerbel R (2002). Antitumor effects in mice of low-dose (metronomic) cyclophosphamide administered continuously through the drinking water. *Cancer Res* **62**, 2731–2735.

[7] Fukushima M, Satake H, Uchida J, Shimamoto Y, Kato T, Takechi T, Okabe H, Fujioka A, Nakano K, Ohshimo H, et al. (1998). Preclinical antitumor efficacy of S-1: a new oral formulation of 5-fluorouracil on human tumor xenografts. *Int J Oncol* **13**, 693–698.

[8] Koizumi W, Narahara H, Hara T, Takagane A, Akiya T, Takagi M, Miyashita K, Nishizaki T, Kobayashi O, Takiyama W, et al. (2008). S-1 plus cisplatin *versus* S-1 alone for first-line treatment of advanced gastric cancer (SPIRITS trial): a phase III trial. *Lancet Oncol* **9**, 215–221.

[9] Kato H, Ichinose Y, Ohta M, Hata E, Tsubota N, Tada H, Watanabe Y, Wada H, Tsuboi M, and Hamajima N (2004). A randomized trial of adjuvant chemotherapy with uracil-tegafur for adenocarcinoma of the lung. *N Engl J Med* **350**, 1713–1721.

[10] Watanabe T, Sano M, Takashima S, Kitaya T, Tokuda Y, Yoshimoto M, Kohno N, Nakagami K, Iwata H, Shimozuma K, et al. (2009). Oral uracil and tegafur compared with classic cyclophosphamide, methotrexate, fluorouracil as postoperative chemotherapy in patients with node-negative, high-risk breast cancer: National Surgical Adjuvant Study for Breast Cancer 01 Trial. *J Clin Oncol* **27**, 1368–1374.

[11] Llovet J, Ricci S, Mazzaferro V, Hilgard P, Gane E, Blanc J, de Oliveira A, Santoro A, Raoul J, Forner A, et al. (2008). Sorafenib in advanced hepatocellular carcinoma. *N Engl J Med* **359**, 378–390.

[12] Klement G, Baruchel S, Rak J, Man S, Clark K, Hicklin D, Bohlen P, and Kerbel R (2000). Continuous low-dose therapy with vinblastine and VEGF receptor-2 antibody induces sustained tumor regression without overt toxicity. *J Clin Invest* **105**, R15–R24.

[13] Pietras K and Hanahan D (2005). A multitargeted, metronomic, and maximum-tolerated dose "chemo-switch" regimen is antiangiogenic, producing objective responses and survival benefit in a mouse model of cancer. *J Clin Oncol* **23**, 939–952.

[14] Wedge S, Ogilvie D, Dukes M, Kendrew J, Chester R, Jackson J, Boffey S, Valentine P, Curwen J, Musgrove H, et al. (2002). ZD6474 inhibits vascular endothelial growth factor signaling, angiogenesis, and tumor growth following oral administration. *Cancer Res* **62**, 4645–4655.

[15] Wang H, Jiang H, Zhou M, Xu Z, Liu S, Shi B, Yao X, Yao M, Gu J, and Li Z (2009). Epidermal growth factor receptor VIII enhances tumorigenicity and resistance to 5-fluorouracil in human hepatocellular carcinoma. *Cancer Lett* **279**, 30–38.

[16] Bocci G, Francia G, Man S, Lawler J, and Kerbel R (2003). Thrombospondin 1, a mediator of the antiangiogenic effects of low-dose metronomic chemotherapy. *Proc Natl Acad Sci USA* **100**, 12917–12922.

[17] Kamat A, Kim T, Landen CJ, Lu C, Han L, Lin Y, Merritt W, Thaker P, Gershenson D, Bischoff F, et al. (2007). Metronomic chemotherapy enhances the efficacy of antivascular therapy in ovarian cancer. *Cancer Res* **67**, 281–288.

[18] Zhang X and Lawler J (2007). Thrombospondin-based antiangiogenic therapy. *Microvasc Res* **74**, 90–99.

[19] Ghiringhelli F, Menard C, Puig P, Ladoire S, Roux S, Martin F, Solary E, Le Cesne A, Zitvogel L, and Chauffert B (2007). Metronomic cyclophosphamide regimen selectively depletes $CD4^+CD25^+$ regulatory T cells and restores T and NK effector functions in end stage cancer patients. *Cancer Immunol Immunother* **56**, 641–648.

[20] Pasquier E, Kavallaris M, and André N (2010). Metronomic chemotherapy: new rationale for new directions. *Nat Rev Clin Oncol* **7**, 455–465.

[21] Bocci G, Nicolaou K, and Kerbel R (2002). Protracted low-dose effects on human endothelial cell proliferation and survival *in vitro* reveal a selective antiangiogenic window for various chemotherapeutic drugs. *Cancer Res* **62**, 6938–6943.

[22] O'Reilly M, Boehm T, Shing Y, Fukai N, Vasios G, Lane W, Flynn E, Birkhead J, Olsen B, and Folkman J (1997). Endostatin: an endogenous inhibitor of angiogenesis and tumor growth. *Cell* **88**, 277–285.

[23] Ebos J, Lee C, Munoz W, Bjamason G, Christensen J, and Kerbel R (2009). Accelerated metastasis after short-term treatment with a potent inhibitor of tumor angiogenesis. *Cell Press* **15**, 232–239.

[24] Hasegawa K, Takayama T, Ijichi M, Matsuyama Y, Imamura H, Sano K, Sugawara Y, Kokudo N, and Makuuchi M (2006). Uracil-tegafur as an adjuvant for hepatocellular carcinoma: a randomized trial. *Hepatology* **44**, 891–895.

[25] Tang T, Man S, Lee C, Xu P, and Kerbel R (2010). Impact of metronomic UFT/cyclophosphamide chemotherapy and antiangiogenic drug assessed in a new preclinical model of locally advanced orthotopic hepatocellular carcinoma. *Neoplasia* **12**, 264–274.

[26] Tran J, Master Z, Yu J, Rak J, Dumont D, and Kerbel R (2002). A role for survivin in chemoresistance of endothelial cells mediated by VEGF. *Proc Natl Acad Sci USA* **99**, 4349–4354.